# Three-dimensional Effects on Unsteady Dynamics and Turbulent Transport Mechanisms of an Impinging Shock Wave/Boundary-layer Interaction

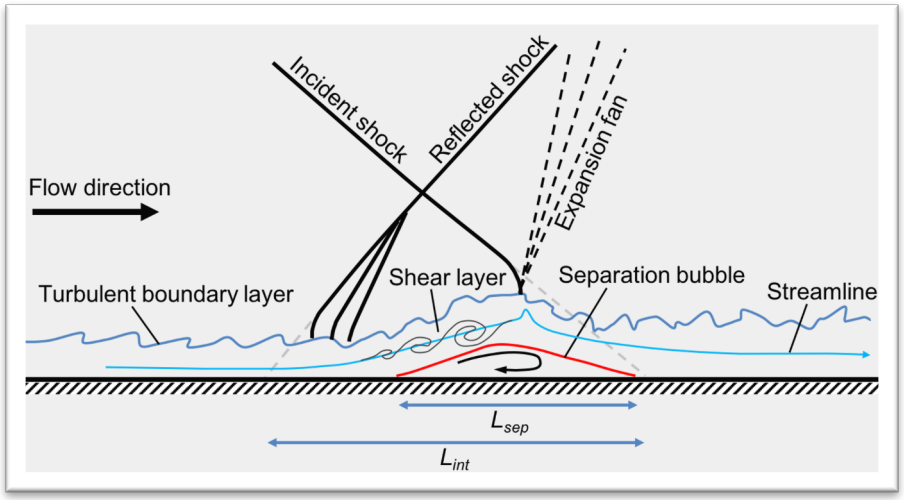
Manan A. Vyas
*NASA Glenn Research Center*
Datta V. Gaitonde
*The Ohio State University*
Dennis A. Yoder
*NASA Glenn Research Center*

Advanced Modeling & Simulation (AMS) Seminar Series
June 2, 2021

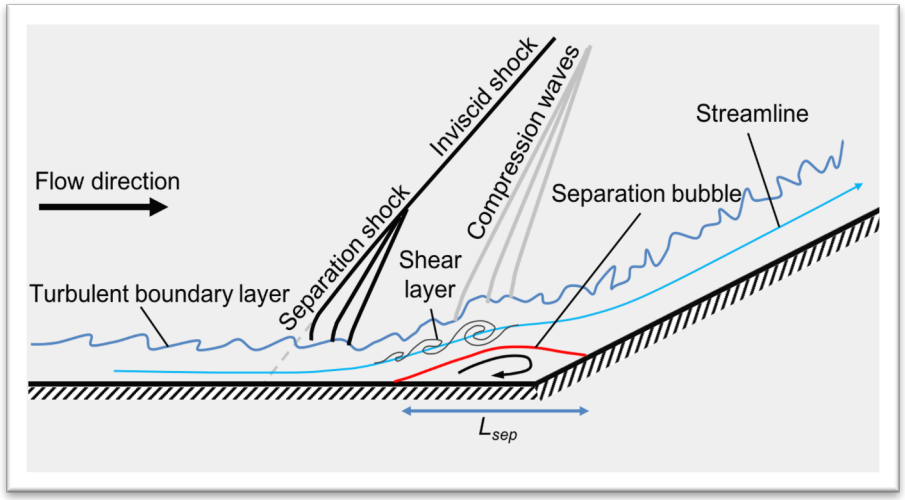
# Outline

- Background
  - Problem and motivation
  - Objectives
  - Details of computational approach
- Comparison with the experimental data
  - Identification of key phenomena in the interaction region
  - Reflected-shock unsteadiness
- New insights into the SBLI and corner regions
  - Secondary flow and corner separation interaction
  - Spectral analysis of volume probes
  - Corner-corner correlation
  - Corner-centerline correlation
- Reynolds-stress transport budgets
  - Streamwise evolution and significant mechanisms
  - Spanwise variation across the interaction region
- Conclusions

# Problem: Canonical 2D SBLIs




**Impinging shock**

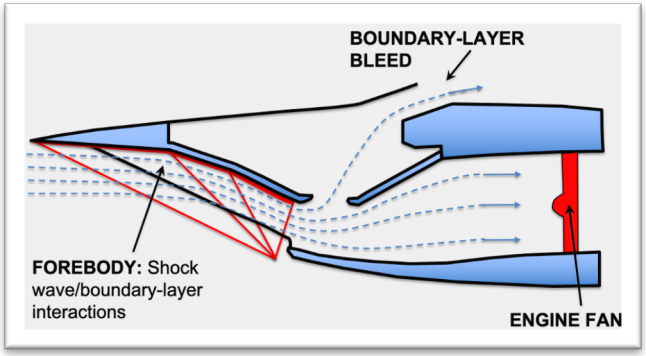


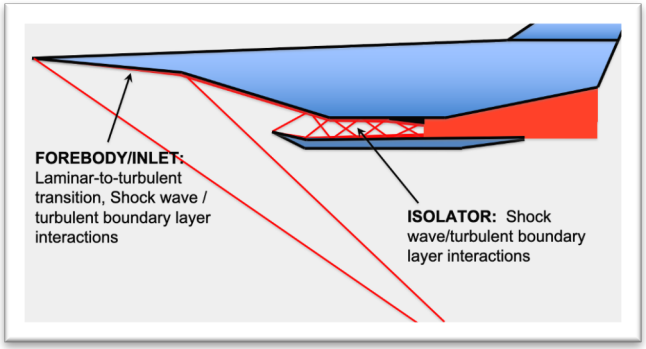

**Compression corner**

- Other canonical configurations: swept ramp, single-fin, double-fin, and double cone.
- Incipiently separated flow correlates with the incoming turbulent boundary layer (BL), whereas fully separated flow correlates with the reflected-shock foot
- Unsteadiness characterized by Strouhal number ($St_{L_{int}} = f L_{int}/U_\infty$)
- Sidewall influence in the form of the corner separation is present for inlets and isolators

# Motivation (1)

- Focus on improved predictions of SBLIs present in propulsion flowpath environment
- 2010 AIAA SBLI prediction workshop
  - Turbulence model played a significant role in variations among different RANS solutions
  - **Scale-resolving methods provided promising solutions, but more development needed**
- RANS-based approaches
  - One- and two-equation models
  - Reynolds-stress models
    - **Interest due to its theoretical superiority and ability to predict secondary flows**
- Scale-resolving methods
  - Hybrid RANS/LES
  - Sub-grid scale closures (LES)
  - **Wall-resolved (WR) LES (moderate Reynolds #)**
  - DNS (low Reynolds #)



# Motivation (2)

## Scale-resolving simulations

- Past scale-resolving SBLI simulations have focused on unsteady dynamics
- *Babinsky et al.* [2013] have suggested corner separation induced compression waves as possible source of separation amplification at the centerline
- *Bisek* [2015] and *Poggie and Porter* [2019] studied SBLIs in a compression corner, which included sidewalls

## Budgets and corner studies

- The studies scrutinizing corner region focused on explaining the secondary flow of the second kind – counter rotating vortex pair symmetric about the corner bisector
- Corner bisector budgets were studied by *Huser et al.* [1994] in a DNS of a square duct, while others have studied budgets in boundary layers and channel flows

- *Morgan et al.* [2013] calculated budgets of $\overline{\rho u'' u''}$ and $\overline{\rho u'' v''}$ from an ILES of an SBLI where periodicity in span was assumed

# Motivation (3)

- Limited application of scale-resolving simulations in investigating and validating SBLIs with sidewall effects
  - Secondary flow and corner separation interaction
  - Influence of corner compression waves on the centerline separation
  - Correlation between the corner and centerline
  - Corner-corner correlation
- Comprehensive Reynolds-stress budgets analysis of an SBLI still absent in the literature
  - More validation of the budgets in undisturbed corner
  - Calculating budgets within a separated corner
  - Assessing spanwise variation in the budgets
- These constitute as gaps in the current understanding of SBLIs and ability to improve predictive capability of the future simulations depend on it.

# Objectives

1. Full-span wall-resolved LES at experimental Reynolds number and validation against the data
2. Examination of the corner compression waves as a potential mechanism behind amplification of the centerline separation and the source of three-dimensionality
3. Investigate the unsteady characteristics by employing spectral analysis
   - Within the SBLI to identify key phenomena in the low-, intermediate-, and high-frequency ranges
   - Examine the corner unsteadiness and corner-centerline connection to ascertain the influence of corner dynamics on the centerline
4. Conduct a comprehensive analysis of the exact Reynolds-stress transport budgets
   - Along the centerline and the corner bisector to elucidate transport mechanisms critical in the SBLI and corner regions
   - Create a database of turbulence quantities that could be used to validate modeling assumptions or inform model development using machine learning or artificial intelligence techniques

# Solver: FDL3DI

- Developed at AFRL
- Implicit large-eddy simulations with wall-resolved mesh, i.e., no explicit modeling of the subgrid scales
- Sixth-order compact spectral-like scheme of *Lele* [1992]
- Eighth-order low-pass Padé-type non-dispersive spatial filter is applied after each sub-iteration to maintain stability
  - Thus, providing an implicit subgrid closure
- Implicit time integration with *Beam-Warming* [1978] using two sub-iterations and approximate factorization
- WENO-type Pressure-based shock sensor using *Roe* scheme [1981] with *van Leer* limiter [1979] at shock location demonstrated by *Visbal and Gaitonde* [2005]
- Unsteady inflow was provided using Digital Filter method
  - Originally proposed by *Klein et al.* [2003], where the filtering was performed in 3D space
  - Closely follows works of *Xie and Castro* [2008], *Touber and Sandham* [2009], and *Adler et al.* [2018]. Here it is applied in 2D form at the inflow plane

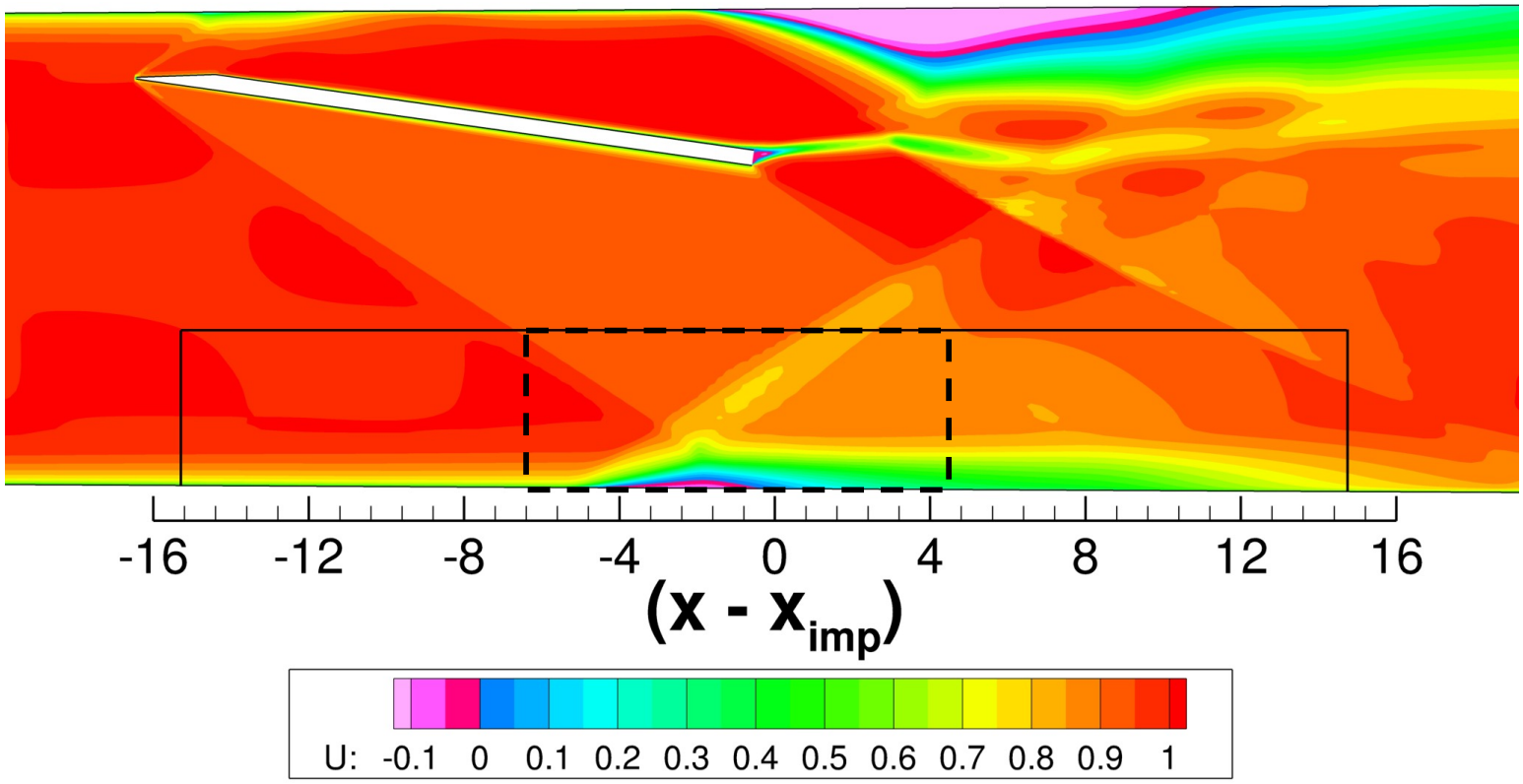
# Inflow conditions

- Revolutionary Computational Aerosciences sub-project's secondary standard test case for propulsion
- Mach 2.29 Impinging SBLI, IUSTI (*Dupont et al.* [2008])
  - PIV, LDA, and HWA measurements at the centerline
  - Pressure spectra
- Nominal Inflow conditions

| | | |
|---|---|---|
| Wedge angle | 8 | degree |
| $M_\infty$ | 2.29 | |
| $U_\infty$ | 545 | m/s |
| $P_0$ | 50663 | Pa |
| $T_0$ | 300 | K |
| $\delta_{99}$ | 11 | mm |
| $Re_\delta$ | 53420 | |
| $Re_\theta$ | 4600 | |

# Computational setup: BCs

- Full-span boundary conditions




- Shock imposed using a freestream plane extracted from a RANS solution
- No-slip adiabatic wall

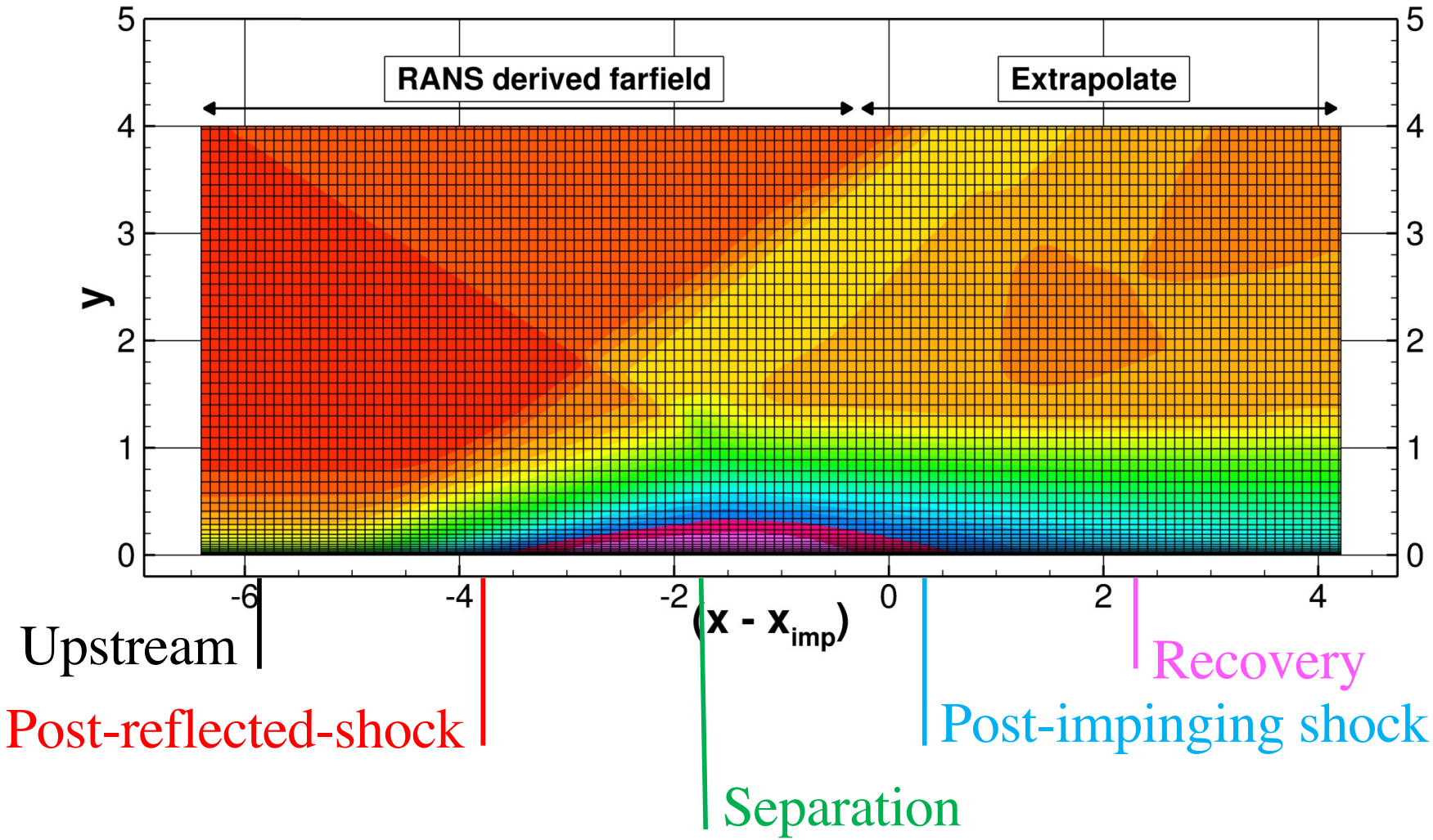
# Computational Setup: Grid

- Periodic and Full-span cases

| | Periodic (baseline) | Full-span |
|---|---|---|
| X x Y x Z in $\delta_0$ | 30 x 4 x 5 | 30 x 4 x 17 |
| $N_x$ x $N_y$ x $N_z$ | 1025 x 257 x 257 | 1025 x 395 x 1485 |
| $\Delta x^+$ | 15.0 | 15.0 |
| $\Delta y_w^+$ | 0.68 | 0.68 |
| $\Delta z_w^+$ | n. a. | 0.68 |
| $\Delta z_c^+$ | 13.0 | 10.0 |

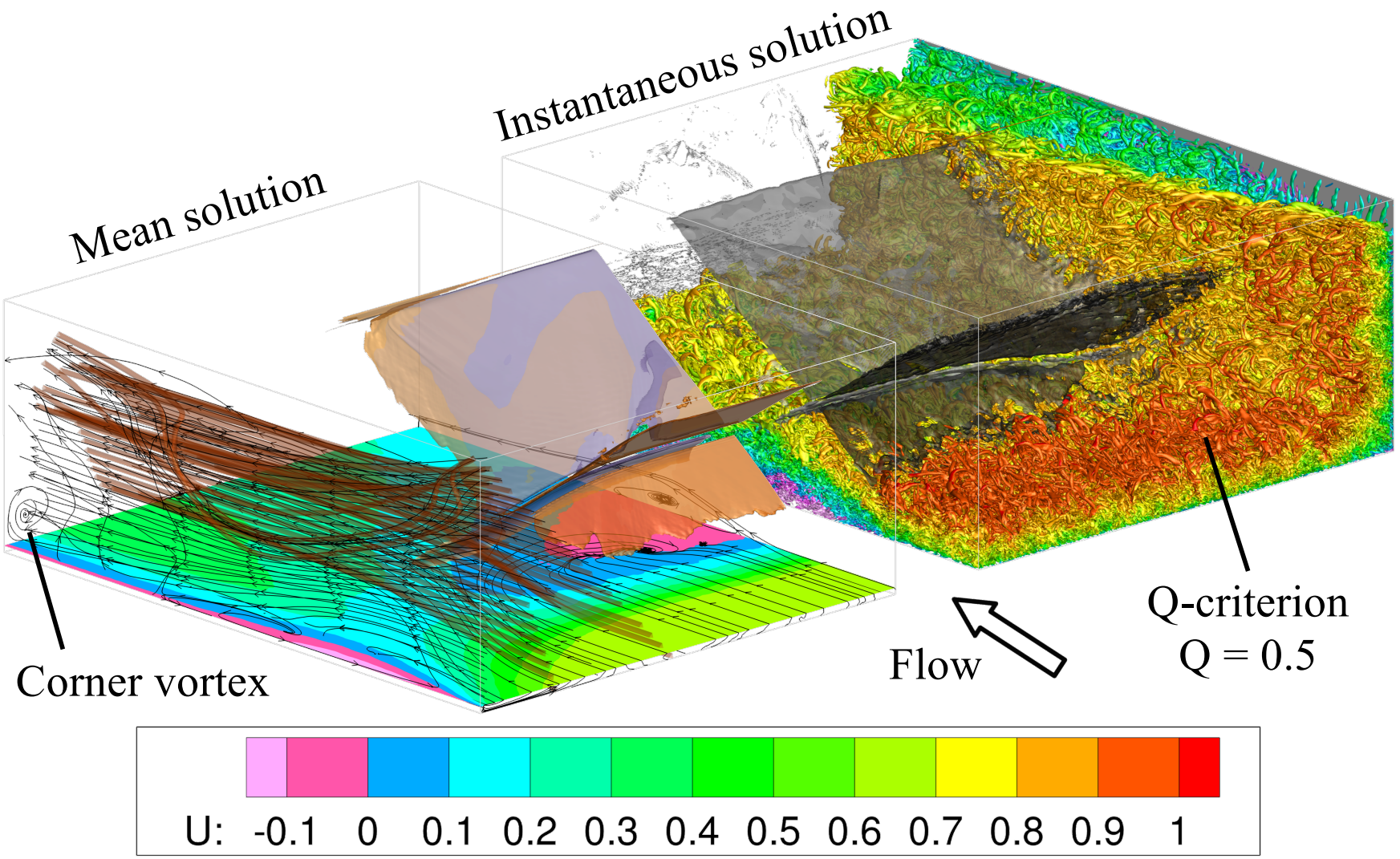
- Studied sensitivity to mesh resolution in earlier periodic SBLI work
  - Baseline mesh was refined in x (x-Refine), y (y-Refine), and z (z-Refine) by doubling the number of grid point
- Full-span mesh was developed based on the resolution requirements established in the periodic work

# Computational setup: BCs and Grid

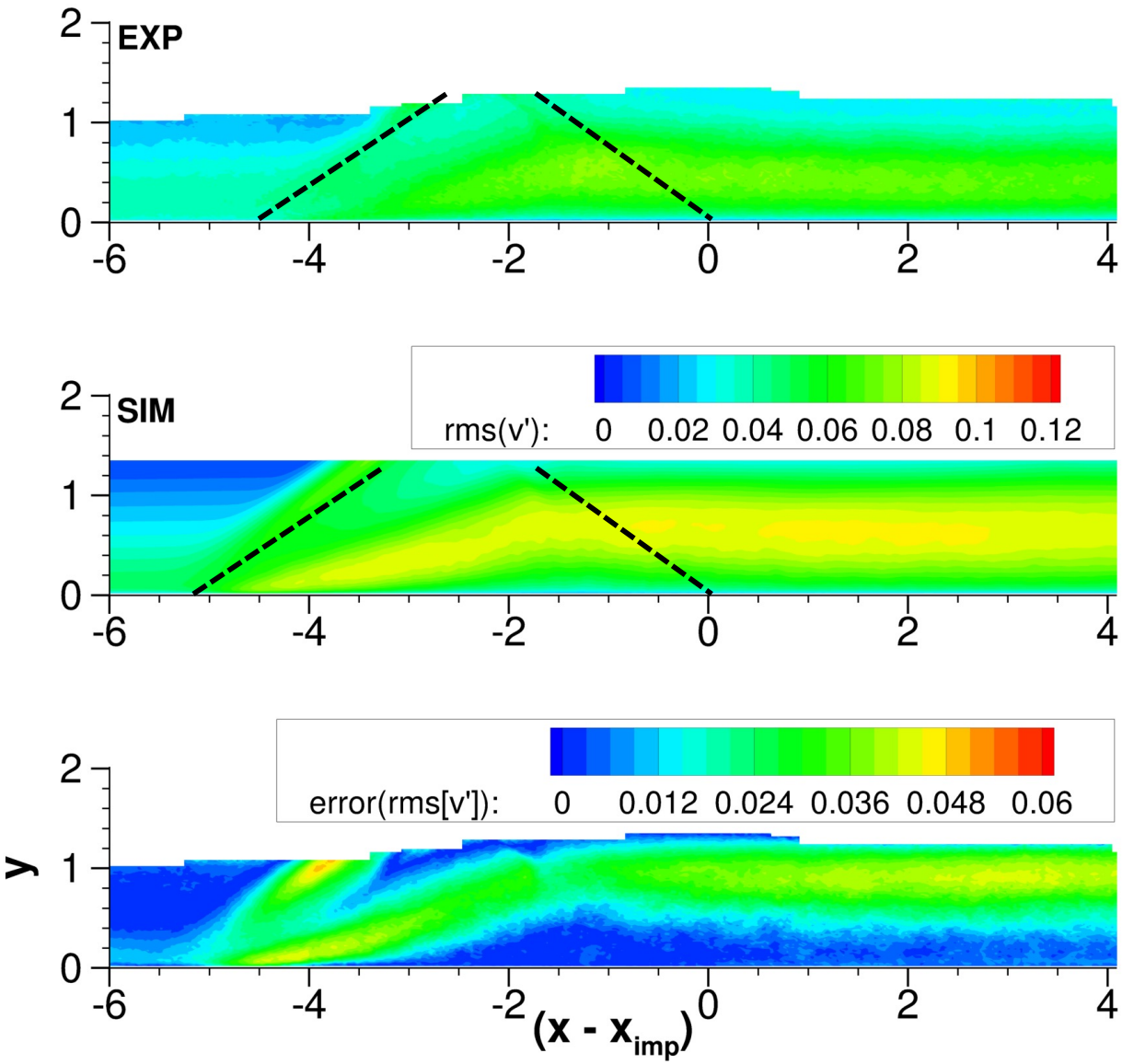



- Every 4th point in x-direction and 8th in y-direction shown

# Flow topology

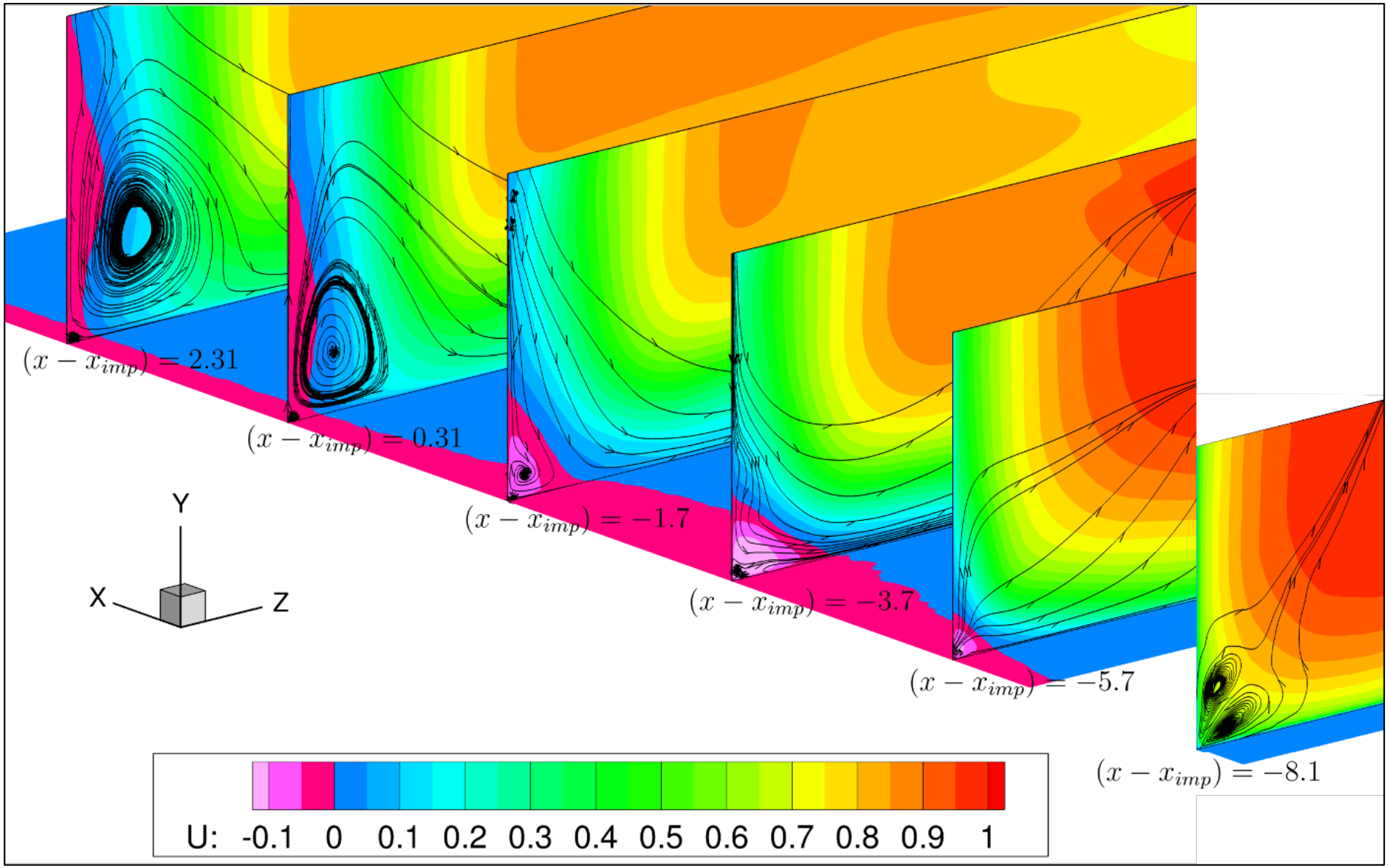


# Stresses and error



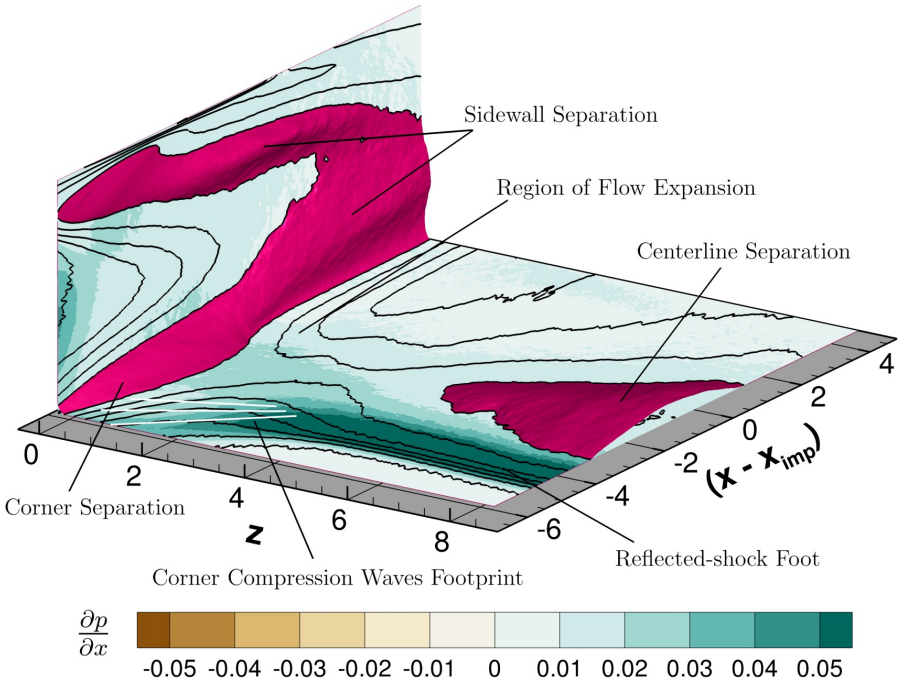

- Marginal overprediction of the interaction length: $L_{exp} = 4.60$ vs $L_{cfd} = 5.20$
- $u'_{rms}$
  - Mismatch in the outer portion of the incoming boundary layer
  - A potential cause of the larger separation
- $v'_{rms}$
  - Mismatch in the inner portion of the incoming boundary layer
- $-\overline{\rho u'' v''}$
  - Secondary error band emanating from the start of the separation bubble

# Corner flowfield (1)



# Corner flowfield (2)

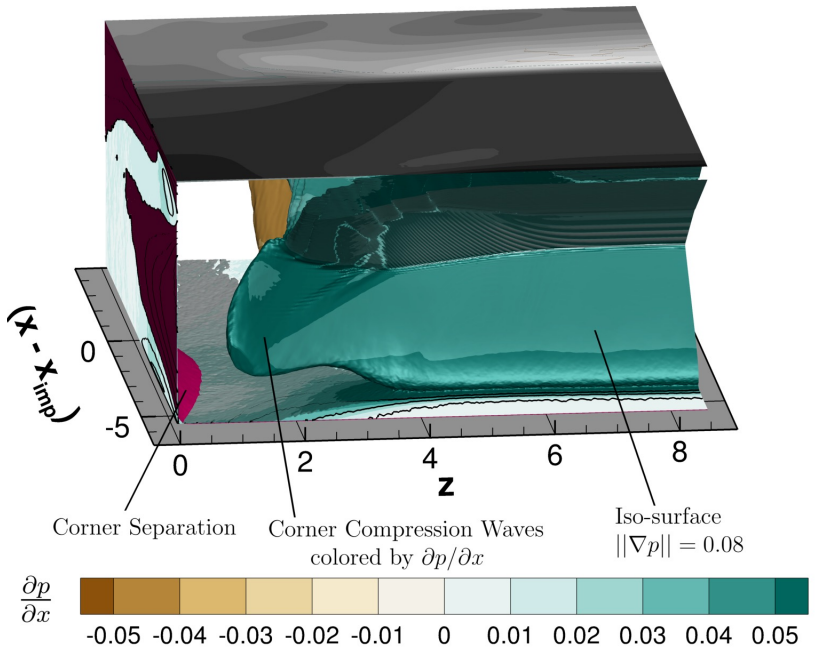
## Corner separation



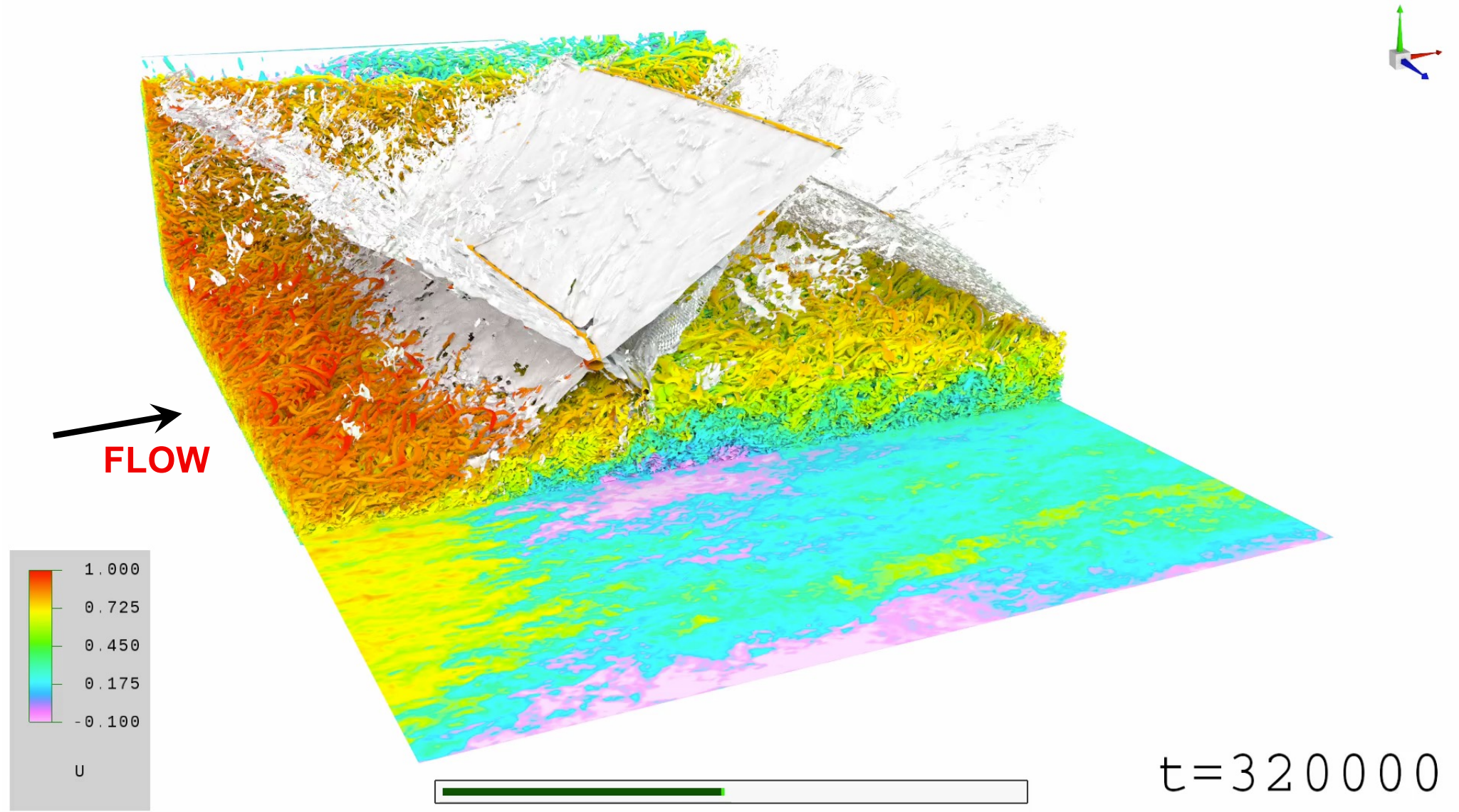

- Symmetric growth of the corner separation up to the crest, but then biased towards sidewall

## Compression waves

- Iso-surface of the pressure gradient shows the compression waves emanating from the corner

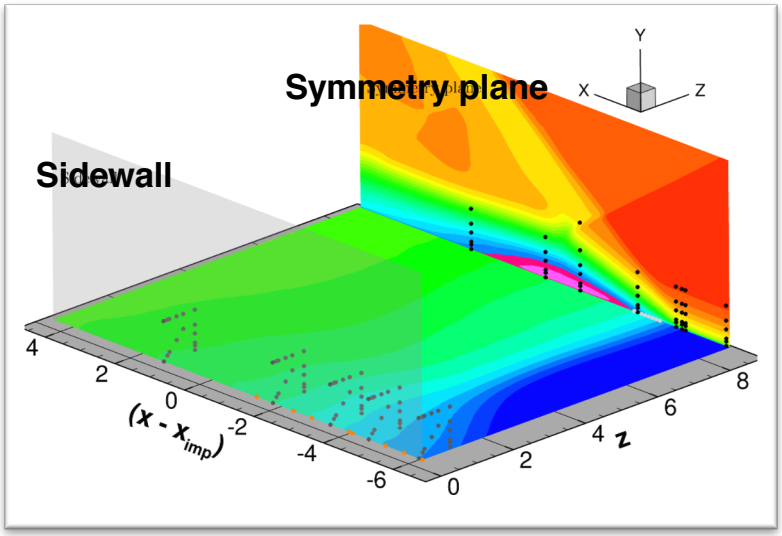


# High frequency animation (2.7 MHz)

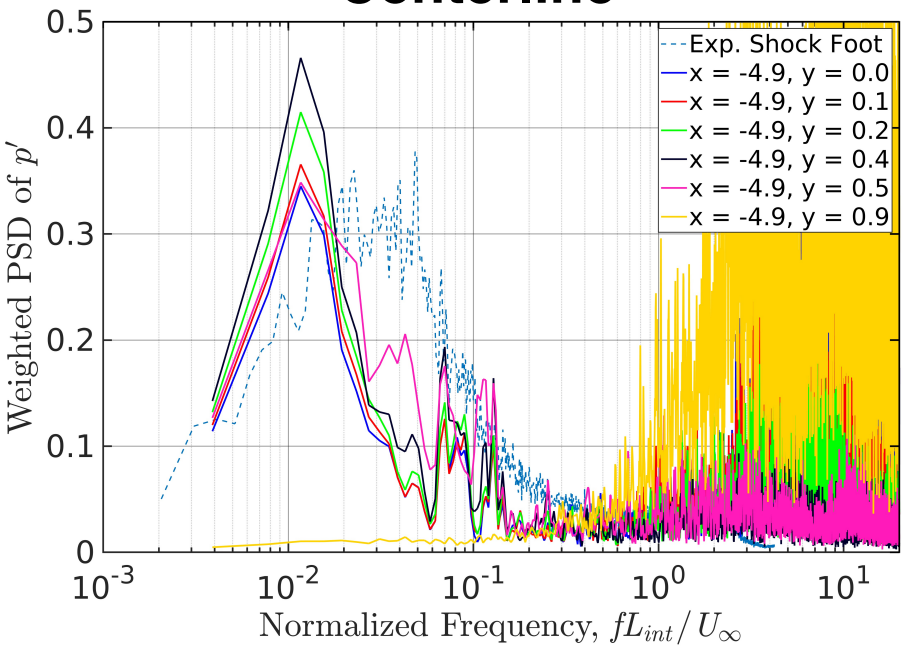


# Low-frequency dynamics

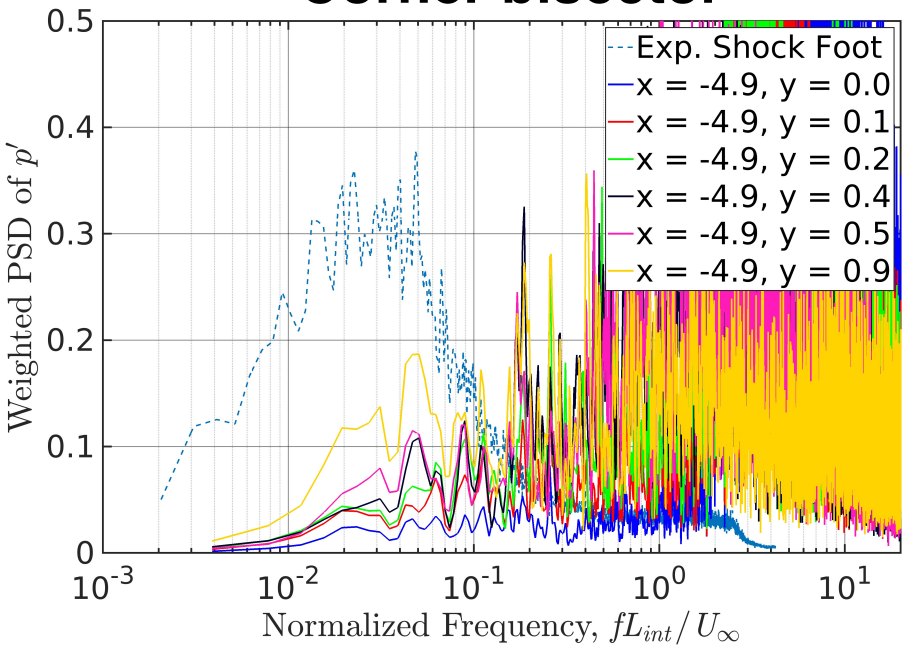
- Strouhal number (based on $L_{int}$) peaked at $St_L \sim 0.015$ (sim) versus $St_L \sim 0.03$ (exp)
- Corner bisector shows coherence with the centerline in the intermediate-frequency range and several narrowband peaks




## Centerline

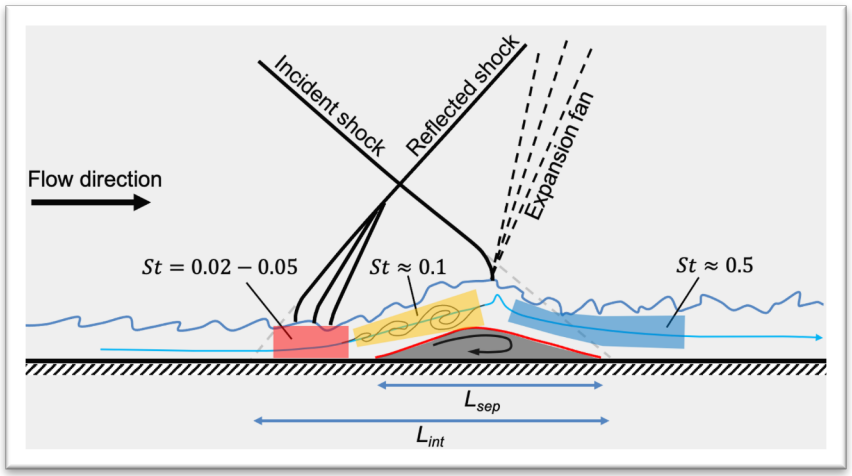



## Corner bisector

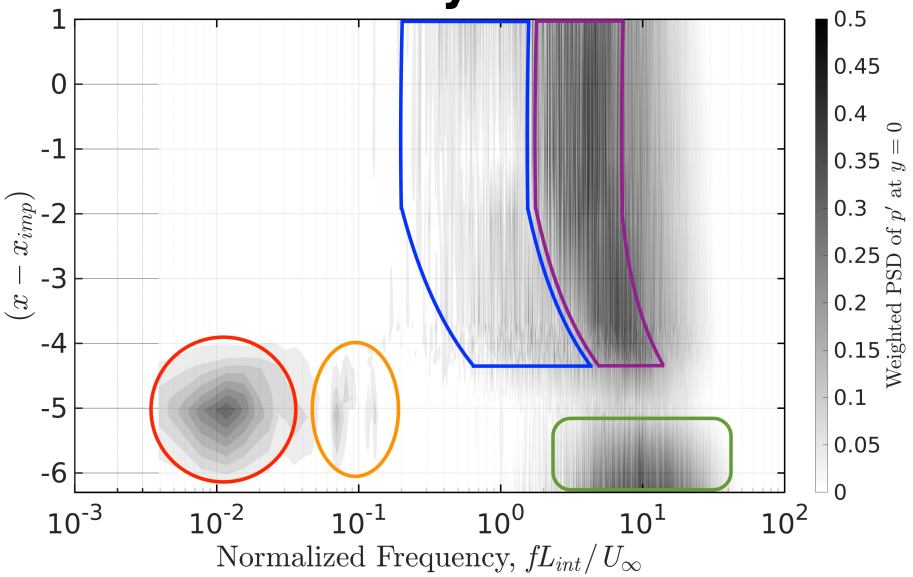


# Dynamics modulating the separation

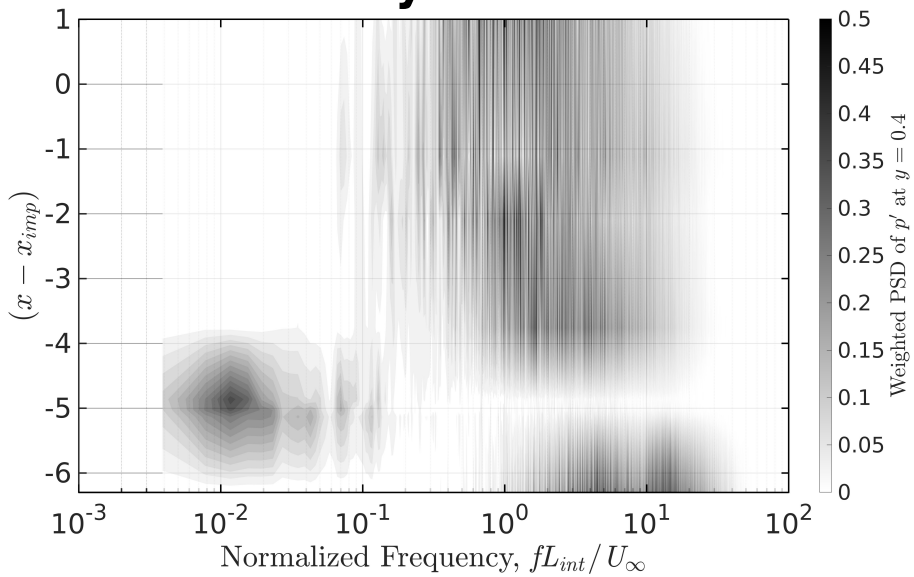
- Energetic scales in the intermediate- ($St_{L_{int}} \approx 0.06 - 0.2$) and high-frequency ($St_{L_{int}} \approx 0.2 - 2.0$) scales are more apparent in the volume probes
- These correspond to the shear-layer development and Kelvin-Helmholtz shedding, respectively




**y = 0**

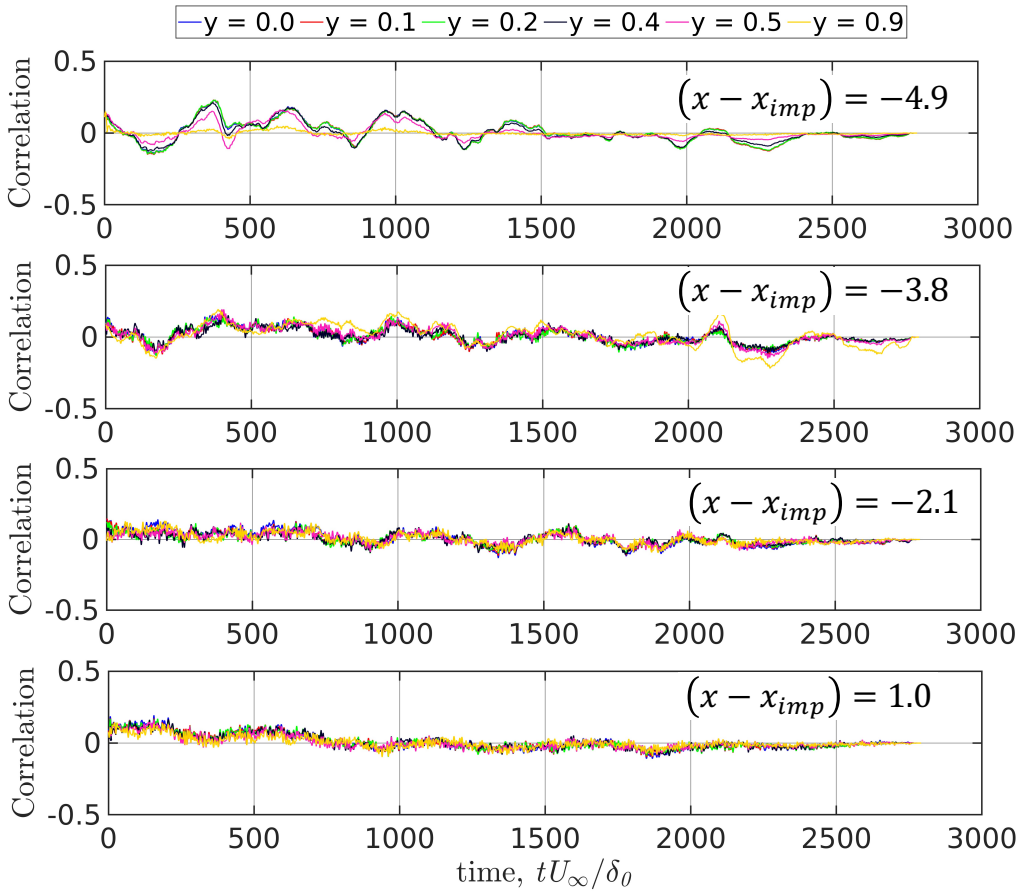


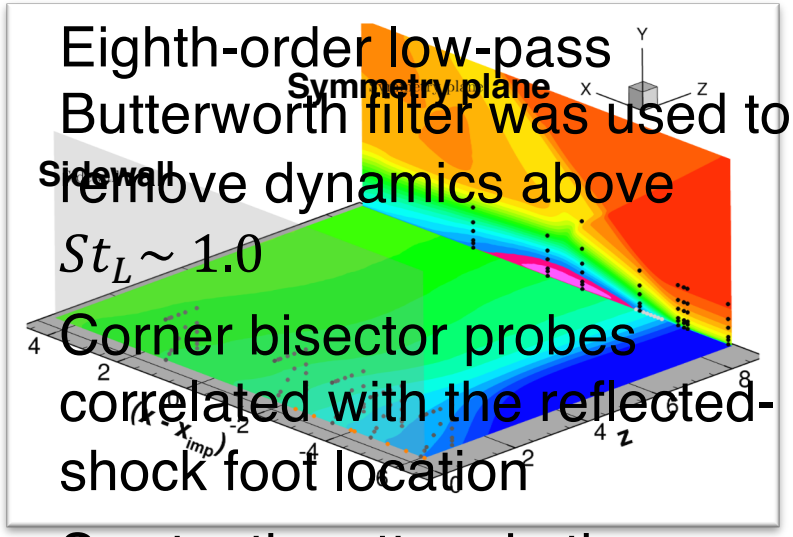

**y = 0.4**



# Corner-centerline correlation

**First probe**
$y = z = 0.4 \quad (x - x_{imp}) = -2.1$

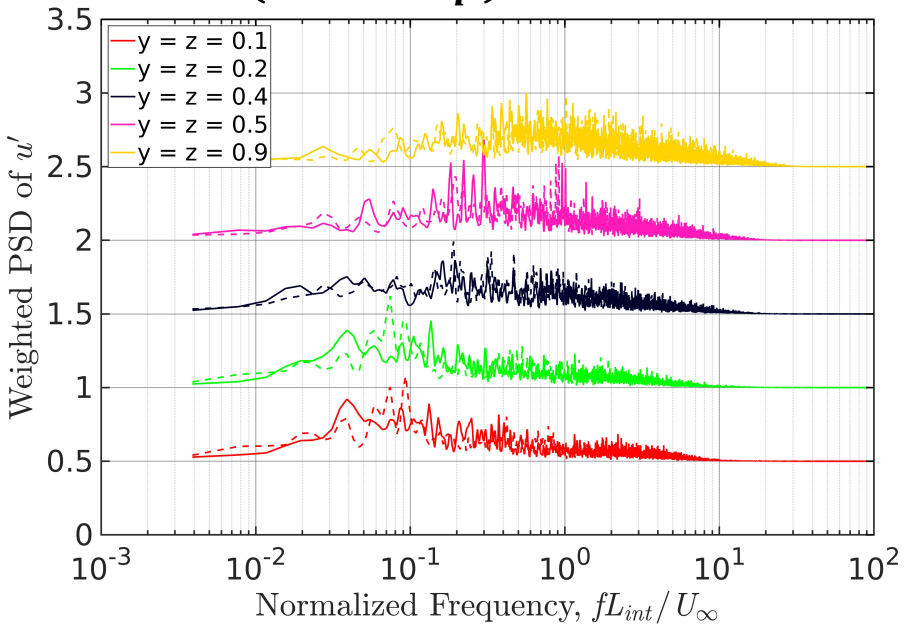


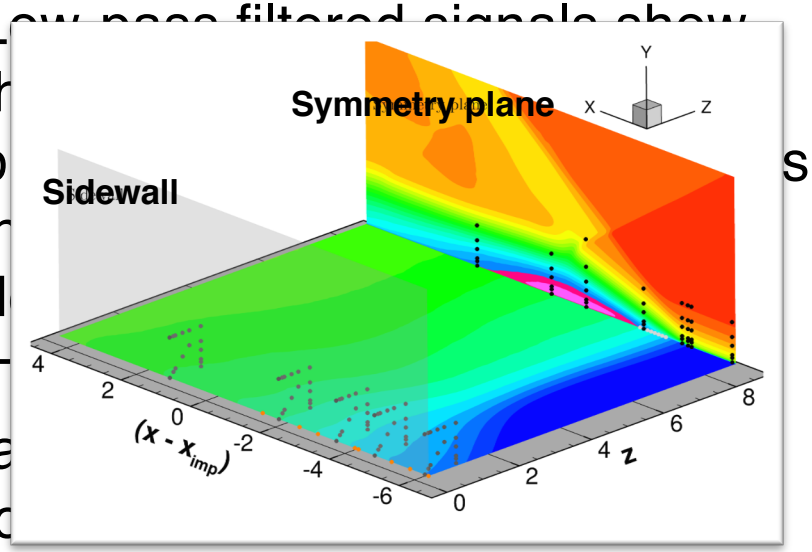

- Eighth-order low-pass Butterworth filter was used to remove dynamics above $St_L \sim 1.0$
- Corner bisector probes correlated with the reflected-shock foot location
- Sawtooth pattern in the correlation corresponds to the forward and aft oscillations of the reflected-shock foot
- Week correlation between the corner region and the centerline at the same streamwise location

# Corner-corner correlation

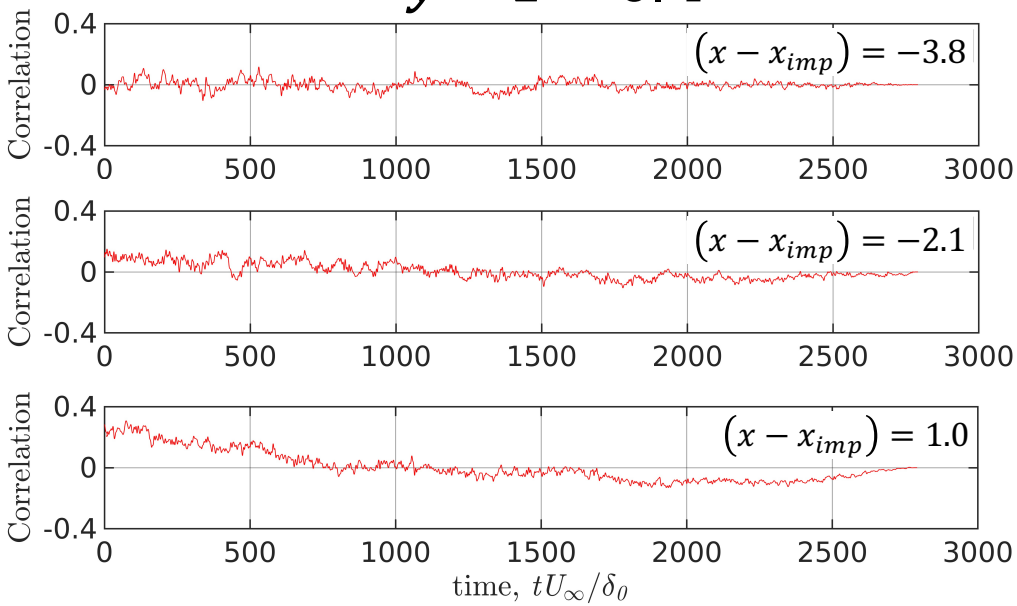
$(x - x_{imp}) = 1.0$




- L… filtered signals show
  th…
  p… s
  in…
  d…
- T…
  la…
  fo…




$y = z = 0.4$




- Within the separated corner region, energetic intermediate-frequency scales were present
- Probes from opposite corners exhibit similar unsteady dynamics

# Reynolds-stress transport equation

- The Reynolds-stress transport equation:

$$\frac{\partial}{\partial t}(\overline{\rho u_i'' u_j''}) + \frac{\partial}{\partial x_k}(\overline{\rho u_i'' u_j'' \tilde{u}_k}) = \mathcal{P}_{ij} + \mathcal{D}_{ij} - \bar{\rho}\epsilon_{ij} + \Pi_{ij} + \mathcal{M}_{ij}$$

$$\mathcal{P}_{ij} = -\overline{\rho u_i'' u_k''}\frac{\partial \tilde{u}_j}{\partial x_k} - \overline{\rho u_j'' u_k''}\frac{\partial \tilde{u}_i}{\partial x_k} \qquad \text{Production}$$

$$\mathcal{D}_{ij}^{\nu} = \frac{\partial}{\partial x_k}\left[\overline{u_i'' t_{kj} + u_j'' t_{ki}}\right] \qquad \text{Molecular Diffusion}$$

$$\mathcal{D}_{ij}^{T} = -\frac{\partial}{\partial x_k}\left[\overline{\rho u_i'' u_j'' u_k''}\right] \qquad \text{Turbulent Diffusion}$$

$$\mathcal{D}_{ij}^{P} = -\frac{\partial}{\partial x_k}\left[\overline{p' u_i''}\delta_{jk} + \overline{p' u_j''}\delta_{ik}\right] \qquad \text{Pressure Diffusion}$$

$$\Pi_{ij} = \overline{p'\left(\frac{\partial u_i''}{\partial x_j} + \frac{\partial u_j''}{\partial x_i}\right)} \qquad \text{Pressure Strain}$$

$$\bar{\rho}\epsilon_{ij} = \overline{t_{ki}\frac{\partial u_j''}{\partial x_k}} + \overline{t_{kj}\frac{\partial u_i''}{\partial x_k}} \qquad \text{Dissipation}$$

$$\mathcal{M}_{ij} = \overline{u_i''}\left(\frac{\partial \bar{t}_{kj}}{\partial x_k} - \frac{\partial \bar{p}}{\partial x_j}\right) + \overline{u_j''}\left(\frac{\partial \bar{t}_{ki}}{\partial x_k} - \frac{\partial \bar{p}}{\partial x_i}\right) \qquad \text{Mass Flux}$$

# Sum and inner scaling

- Budget sum should be zero if production, transfer, and dissipation mechanisms that govern the energy cascade are appropriately captured

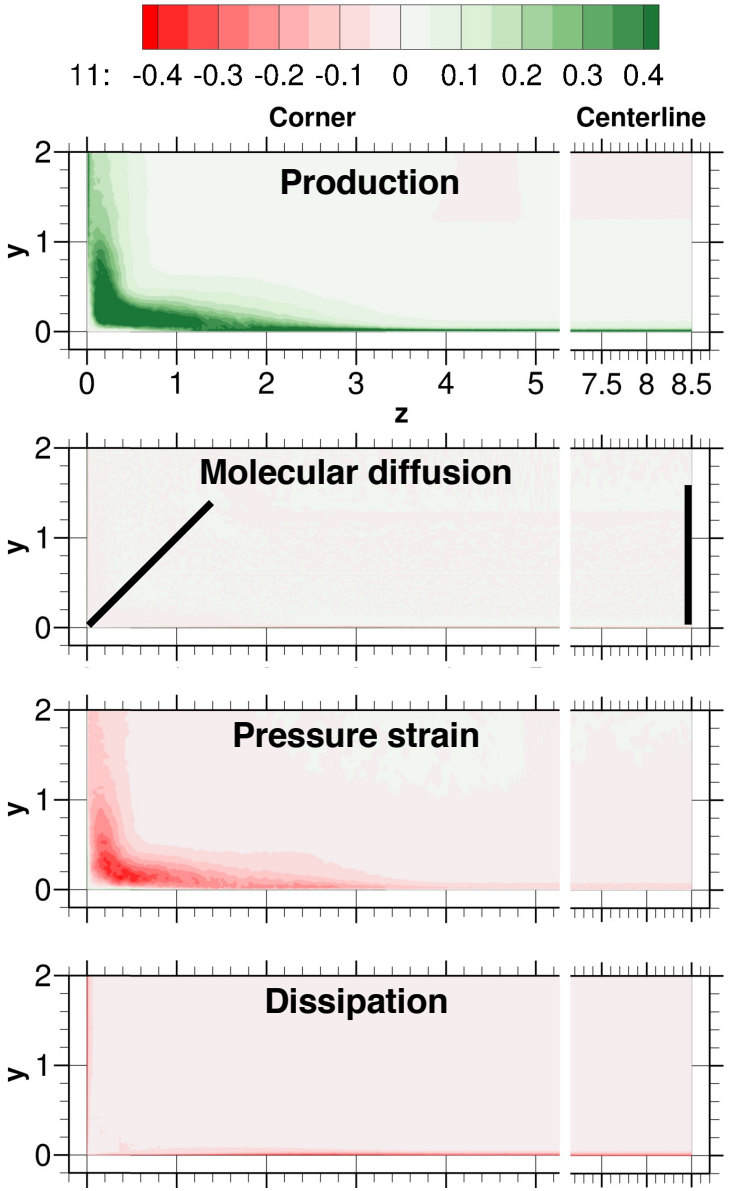
$$\text{Sum} = \mathcal{P}_{ij} + \mathcal{D}_{ij} - \bar{\rho}\epsilon_{ij} + \Pi_{ij} + \mathcal{M}_{ij} - \frac{\partial}{\partial x_k}(\overline{\rho u_i'' u_j''}\tilde{u}_k) = 0$$

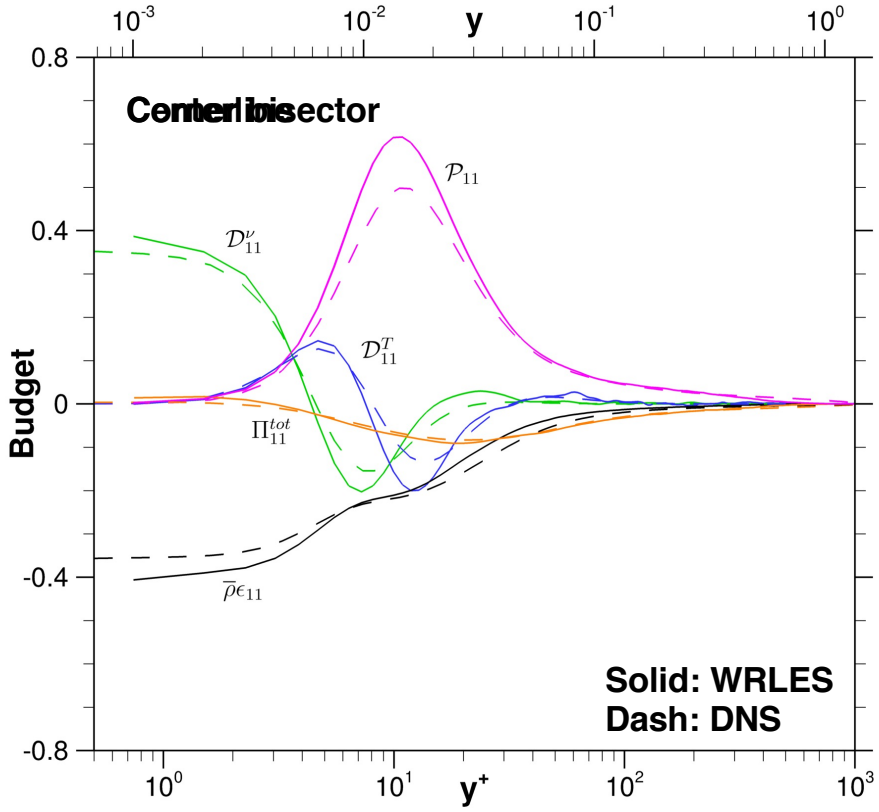
- To calculate the sum, the unsteady term was assumed to be zero, while this was reasonable in the undisturbed boundary layer, such an assumption would not hold in the interaction region
- But the sum is indicative of the unsteady term behavior

$$\frac{\partial}{\partial t}(\overline{\rho u_i'' u_j''}) = \text{Sum} + \text{error}$$

- Inner scaling $(\rho_w u_\tau^4/\nu_w)$ at $(x - x_{imp}) = -5.7$ was used for normalizing budgets at all locations downstream

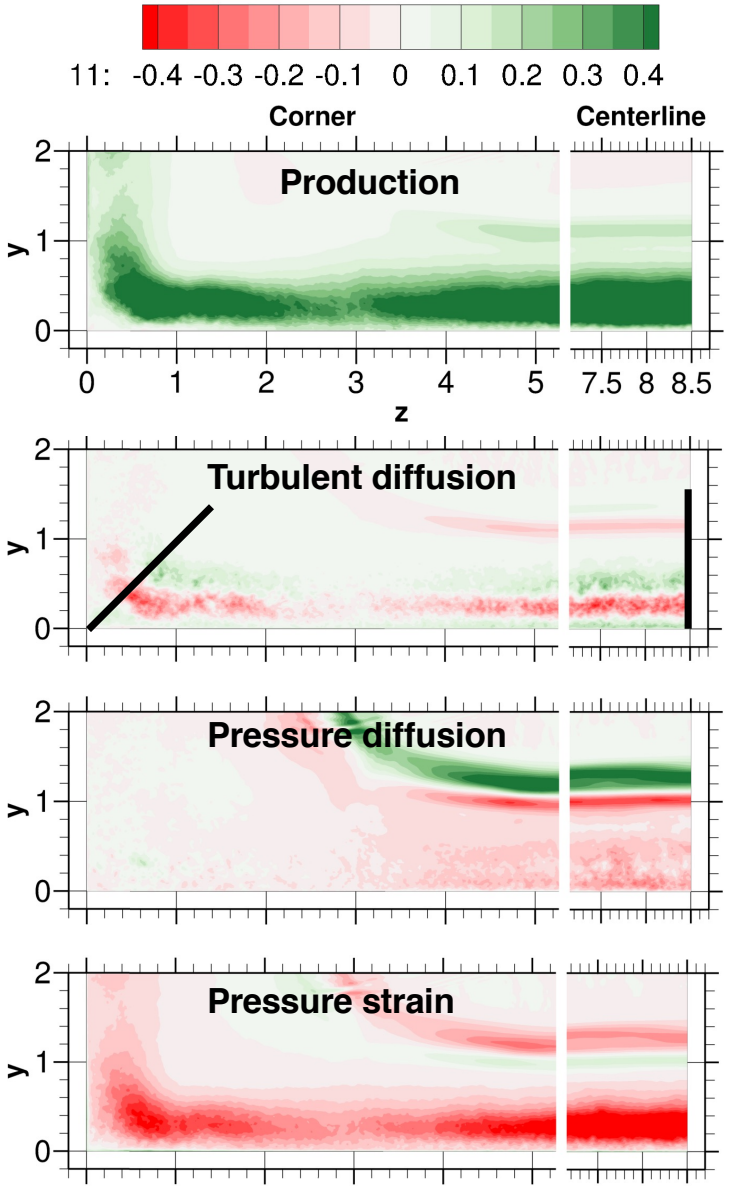
# Upstream: $\overline{\rho u'' u''}$

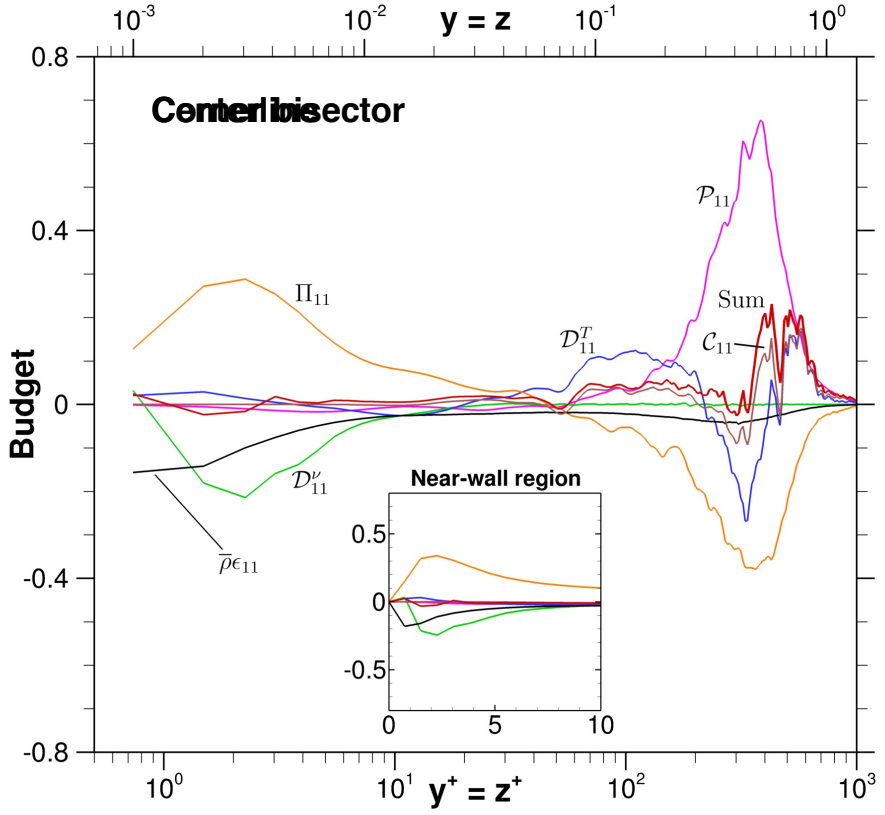



- Centerline: The upstream budgets validated against the turbulent BL DNS
- Corner bisector: The rise in production within the log-law region due to the high velocity gradients caused by the growing separation bubble

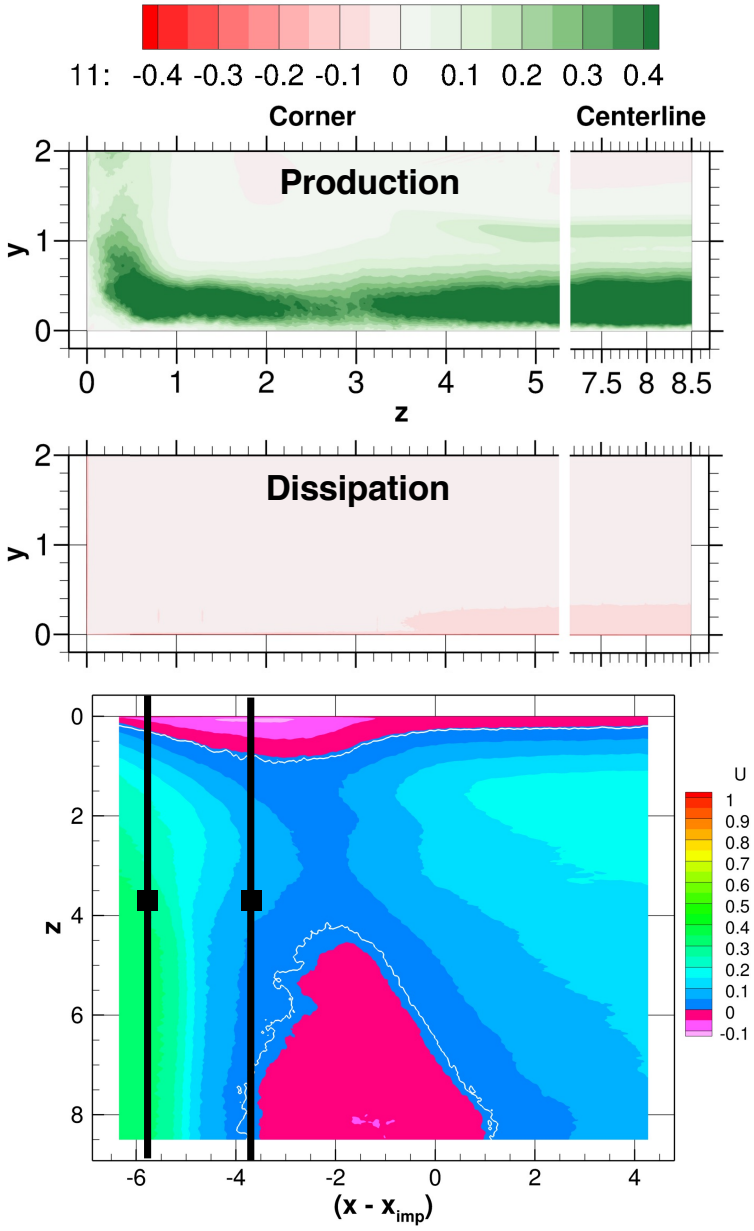
# Post-reflected shock: $\overline{\rho u'' u''}$

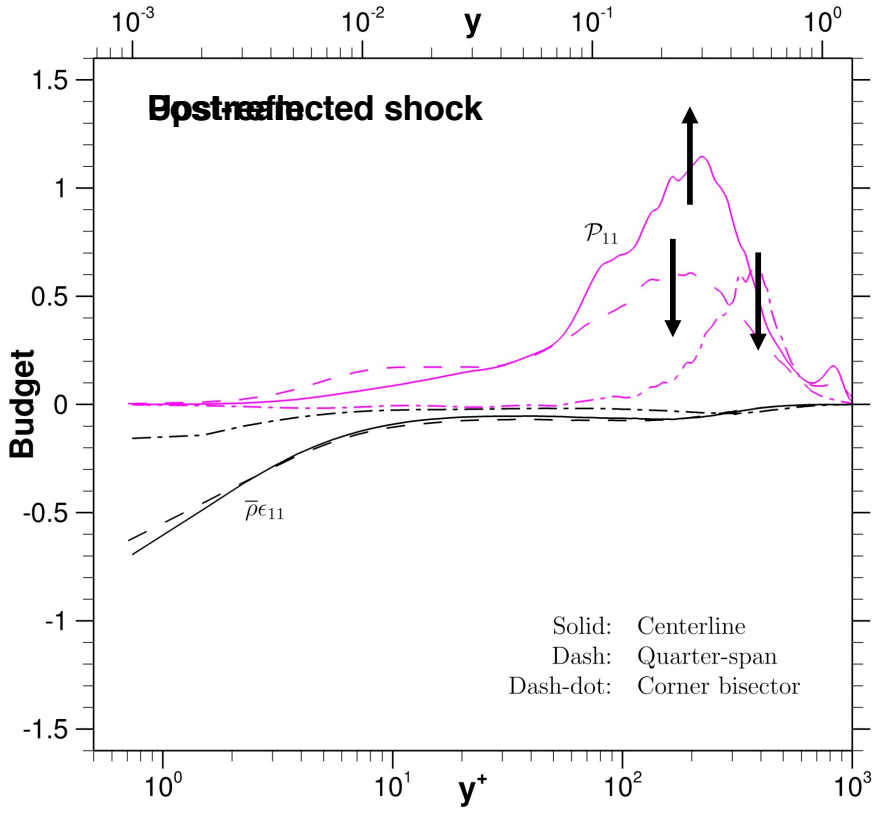



- Centerline: Pressure diffusion was important at the reflected-shock foot and in its downstream vicinity
- Corner bisector: Small reduction in mechanisms and increase in unsteadiness

# Span variation: $\overline{\rho u'' u''}$




- Upstream mechanisms fall in two categories, but downstream of the reflected shock, three behaviors emerge
- Gain in production more complex, due to attached flow between the centerline and corner separation

# Conclusions (1)

1. WRLES approach was shown to be well suited for low to moderate Reynolds number flows and provided DNS-like predictions in the resolved regions
2. The digital filter inflow generation technique was found to be robust in achieving equilibrium-like turbulent boundary layer and suitable for secondary flow development
3. Provided evidence that the sidewall corner separation and the resulting compression waves amplify the separation bubble size
4. The corner-centerline correlations identified that a significant portion of the flowfield was correlated with the forward and aft oscillations of the reflected-shock foot
5. The corner-corner correlations found the opposing corners to be either positively correlated, uncorrelated, or negatively correlated

# Conclusions (2)

6. Provided a comprehensive investigation of the Reynolds stress budgets and other relevant turbulence quantities across the span to elucidate transport mechanisms critical in the SBLI region
7. Revealed the significance of the pressure-diffusion mechanism to the reflected-shock foot
8. Highlighted the dissimilar behavior of diffusion mechanisms, which strengthens the argument to model these mechanisms separately
9. Developed a database of the Reynolds-stress transport mechanisms that model developers can use with traditional or novel methods like machine learning and artificial intelligence to enhance current models or device new modeled terms

# Acknowledgements


- Support of NASA's Transformational Tools and Technologies Project within the Transformative Aeronautics Concepts Program under the Aeronautics Research Mission Directorate.
- Computational resources provided by the NASA High-End Computing Program through the NASA Advanced Supercomputing Division at Ames Research Center.

Questions?

Contact information

Manan A. Vyas

manan.vyas@nasa.gov